Computational Materials Science 149 (2018) 397–408

Contents lists available at ScienceDirect

Computational Materials Science

journal homepage: www.elsevier.com/locate/commatsci

Electron-phonon scattering and Joule heating in copper at extreme cold temperatures☆

Tingyue Lan[a], Tarek Ragab[b], Cemal Basaran[a,*]

[a] Electronic Packaging Lab, University at Buffalo, SUNY, Buffalo, NY 14260, United States
[b] Arkansas State University, State University, AR 72467, United States

ARTICLE INFO

Keywords:
Electron-phonon interaction
Scattering rate
Joule heating
Copper
Extreme cold temperatures

ABSTRACT

A quantum mechanical model has been used to calculate the full electron-phonon scattering rates in pure copper at extreme cold temperatures. The proposed model uses Fermi's Golden rule, specific to each scattering mechanism and wave vector state, providing more accuracy and more details than the widely used empirical third power rule for scattering rates. The empirical third power rule is actually only valid in the low-temperature limit. The results are in good agreement with existing experimental data and theoretical calculations with the assumption that the wave vector of a phonon is much larger than the wave vector of an electron ($q \gg k$) and three-dimensional density of states converted to one-dimensional density of states to reduce calculation burden by orders of magnitude. The energy generated by Joule heating is calculated using the proposed model and compared with the experimental data from the literatures. Although the results presented are specific to copper, the method is directly applicable to other metals. In addition, the proposed model can be used to study the thermal properties of copper wires in high temperature superconductor power cable applications.

1. Introduction

High temperature superconductors (HTS) were first discovered in 1986 [1], with applications in motors, generators and transmission lines [2]. The second-generation (2G) HTS wires are commercially available in copper, brass and stainless steel laminate which are used in HTS power cables and other applications. The 2G HTS wires are conducting with resistance 100 times less than copper wires of similar dimensions, and providing significantly greater power throughput and efficiency as well as high strength and stability with outstanding bend tolerance with reduced size and weight [3,4]. However, to construct a single kilometer of HTS power cable, more than 400 km of HTS wire [5] is needed. Although HTS cables have great advantages in utility power networks or in commercial and industrial applications [4], very high cost is one of the major limiting factors for broad commercialization [5].

Copper is an indispensable part of the HTS cable. If copper can also be utilized more effectively, the cost of HTS cable will be reduced significantly. Therefore, it is very important to study the properties of copper at extreme cold temperatures. To understand the low temperature electron transport in a comprehensive way, full band electron-phonon scattering rates and Joule heating calculations are needed.

In 1966, Häussler and Welles observed the electron-phonon scattering rate anisotropy in the major symmetry directions of copper from cyclotron resonance data [6]. It was found that the total electron-phonon scattering rate $\nu_{ep}(\vec{k},T)$ changes linearly with the cube of the temperature T in the low-temperature limit ($T \to 0$ K) as shown in Eq. (1) and the scattering coefficient $\beta(\vec{k})$ is found to be ten times smaller on the belly orbits than on the neck orbits.

$$\nu_{ep}(\vec{k},T) = \beta(\vec{k})T^3 \tag{1}$$

The electron-phonon scattering rates in copper at extreme cold temperatures have been studied experimentally [6–14] and theoretically [13,15–20] and similar anisotropic behavior was reported. Energy-averaged scattering coefficient was obtained experimentally having a magnitude in the order of $10^6\ s^{-1}\ K^{-3}$, except for the neck region where it has a magnitude in the order of $10^7\ s^{-1}\ K^{-3}$ at temperature of 1.5–12 K [7–9]. Theoretically, Nowak [15] fitted the energy-averaged scattering rates to the experimental Fermi surface qualitatively. Later, Das [17] obtained total scattering rates (including all mechanisms) at several points on Fermi surface. Although results were coherent with experimental findings, very limited data points (states) were calculated. Khan and his group [20] suggested that the usual $\beta(\vec{k})T^3$ law was only valid below 4 K. Their results did not match well with the

☆ The datasets generated during and/or analysed during the current study are available from the corresponding author on reasonable request.

* Corresponding author.
E-mail address: cjb@buffalo.edu (C. Basaran).

https://doi.org/10.1016/j.commatsci.2018.03.049
Received 20 January 2018; Received in revised form 21 March 2018; Accepted 22 March 2018
Available online 27 March 2018

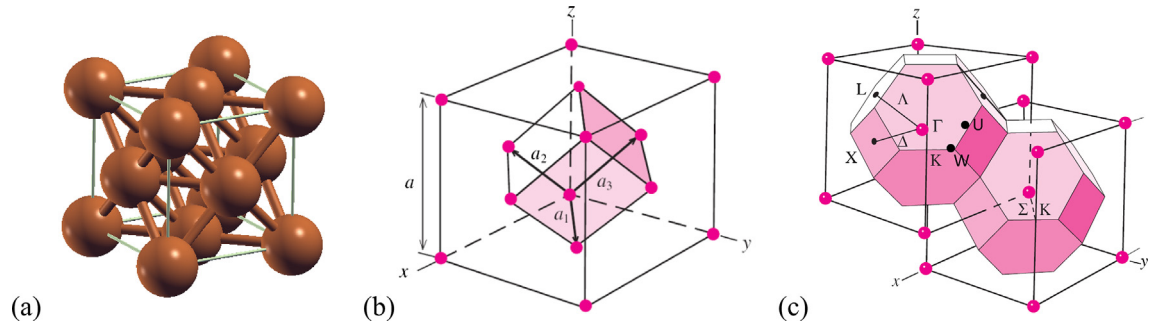

Fig. 1. (a) Crystal structure of copper; (b) Primitive lattice vectors; (c) First Brillouin zone and reciprocal lattice [27].

experimental data and results from other groups.

To better understand scattering mechanisms, instead of using Eq. (1) for an approximate total scattering rate, we employed the accelerated full band model [21] to calculate the point-by-point electron-phonon scattering rates at the Fermi level of copper at extreme cold temperatures. Then based on the energy exchange during the scattering process, the Joule heating was computed utilizing the calculated scattering rates [22–25]. We realize that not all Joule heating is due to electron-phonon scattering. Defect scattering is one of the biggest contributors to Joule heating, however, that is not part of this study.

2. Theory and calculations

2.1. Electronic structure of copper

Copper has a face centered cubic (FCC) lattice (Fig. 1(a)), formed with 29 electrons, 18 in innermost core ($1s^2 2s^2 2p^6 3s^2 3p^6$), 10 in a completely filled d shell ($3d^{10}$), and one in the outermost s shell ($4s^1$) [26]. Fig. 1(b) shows a set of primitive lattice vectors of the FCC lattice. Fig. 1(c) is the reciprocal lattice of the FCC lattice with the first Brillouin zone (BZ). Special high-symmetry points are denoted by Γ, X, and L, while high-symmetry lines joining some of these points are labeled as Λ and Δ [27]. Other points are denoted by K, W and U.

2.2. Energy dispersion relation

The transport properties of solids are closely related to the energy dispersion relations $E(\vec{k})$ and in particular to the behavior of $E(\vec{k})$ near the Fermi level. The closest nine energy bands near Fermi level along the various symmetry axes of the first BZ are calculated using tight-binding model based on the semi-empirical extended Hückel model [28,29]. Although tight-binding quantum molecular dynamics simulations are less accurate than density functional theory (DFT), it is cheap, simple and requires much less computer power which is very important for our three dimensional model. The energy dispersion relation for the chosen atomic orbitals can be obtained by solving the time-independent Schrödinger equation as the eigenvalue problem. The eigenvalues are periodic functions in a reciprocal lattice, hence it can be fully described just within the first BZ [30–32].

Fig. 2 shows the calculated energy bands of copper along the various symmetry axes at 50 K in the first BZ by ATK software package [33]. There are five relatively flat bands lying in a narrow range below Fermi level. These very tightly bound bands are 3d bands and show little wave-vector dependence [34]. The sixth band crosses the Fermi level before reaching the BZ boundary at the X point. It is the 4 s band and has a strong dependence on wave-vector, with an energy range from +4 eV to −5 eV. According to the Fermi Dirac distribution, the most inner part of the first BZ is fully occupied at extreme low temperature, only the electron states near the Fermi energy can participate in scattering events at extreme low temperature. Therefore, the 4 s electron band is the one needs to be considered in this study, since

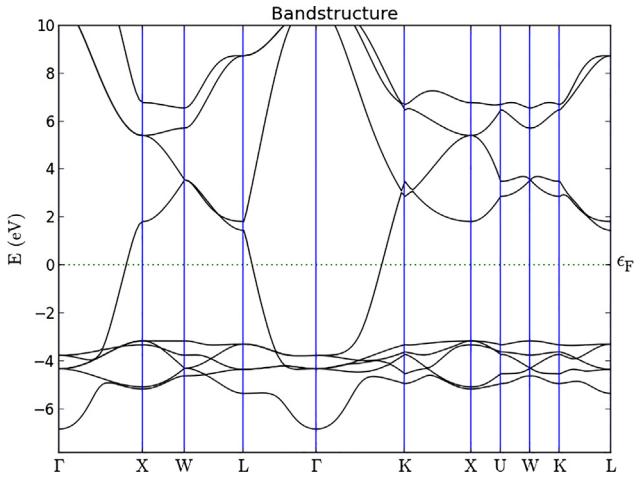

Fig. 2. The energy bands of copper along the various symmetry axes at 50 K in the first BZ.

others are too far away from the Fermi level. Some theoretical calculations via different methods and experimental data along various symmetry lines can be found from Refs. [35–39].

Fermi surface of copper can be obtained by analyzing the energy bands along the major high symmetry directions. Fermi surface of copper within the first BZ is visualized by XCrySDen software package in Fig. 3(a–d). It is nearly a sphere with small areas pulled out in the ⟨1 1 1⟩ directions and making contact with the BZ boundary (Fig. 3(a)). These small areas are the "necks". The Fermi surfaces in different BZs are linked by these necks in the extended zone scheme [40]. Fig. 3(b–d) are the (1 0 0), (1 1 0) and (1 1 1) cross sections of the Fermi surface, respectively.

2.3. Phonon dispersion relations

For electrical transport in copper, three phonon bands are considered: one longitudinal acoustic (LA) band and two transverse acoustic (TA) bands [41–54].

To calculate the phonon dispersion relation, the classical potential model [55,56] is used with the finite difference method in a repeated cell, which is also referred to as frozen-phonon-approach [57,58]. For the classical potential model, consider a crystal with a number of unit cells, which are denoted by l. Each unit cell consists of n particles labelled by k. The Cartesian coordinate indices α and β can be 1, 2 and 3. Then we have Eq. (2) with Φ is the potential energy of the crystal.

$$\Phi_{\alpha,\beta}(l-l',k,k') = \frac{\partial^2 \Phi}{\partial u_\alpha(l,k)\partial u_\beta(l',k')} \tag{2}$$

The displacements of the particles from their equilibrium positions are $u_\alpha(l,k)$.